JOURNAL OF COMPUTATIONAL PHYSICS **133,** 181–185 (1997)
ARTICLE NO. CP975650

NOTE

Large-Scale Simulations on Polymer Melts

Recently the discussion of the behavior of polymer melts in the different time regimes of their diffusion process has attracted new attention [1–3]. Special features during the transition to the center of mass diffusion of the entire chain in the melt were proposed using certain computer simulations and were opposed using other simulations. This recent discussion illuminates a major problem in the area of computer simulations of polymers, namely the size of the system and the duration of the simulation. Concerning the size, the simulations can be divided into two groups, a larger one using 500 to 2,000 repeat units (e.g., [4–10]) and a smaller one using 15,000 to 450,000 units [2, 11–15]. To obtain dense systems the first group puts these monomers into relatively small boxes with periodic boundary conditions. Once more two groups of simulations can be distinguished. The first simulates many, but short, chains. Thus, no entanglements can be found in these polymer systems. The other group prefers long, but few, chains, and some just one chain [6, 9, 10], within the simulation box. They presume that, due to the periodic boundary conditions, self-entanglement of these few chains resembles the situation of many chains. The simulations using low numbers of monomer units are unfortunately on the rise since most heretofore commercially available products have handled at best a few chains within endurable CPU time. The simulation with large numbers of monomers [2, 11–15] can combine both properties, many and long chains, within a reasonably large simulation box. The large simulation (64,000 units) by Brown *et al.* [15] was performed by molecular dynamics. Even the application of state-of-the-art computers and programs limited these simulations to a duration of about 8 ns.

As an example, for the case of melts we will show that a certain system size is vital in obtaining reliable data. Furthermore, large-scale fluctuations will be presented, suggesting that even simulations which are commonly considered long lasting must be treated carefully when extracting structural properties.

The approach presented is based on the well-known three-dimensional bond-fluctuation algorithm [16]. In this coarse-grained lattice model the polymer chains are represented by mutually and self-avoiding walks on a cubic lattice, each monomer occupying eight corners of the unit cell. For more details on the bond-fluctuation model see [16, 17]. The chains in the melts were grown in a random process, ensuring self- and cut-avoiding. Subsequent to the generation the melts were subjected to a random dynamics for a duration of 1,000,000 Monte Carlo steps (MCS). One Monte Carlo step denotes one attempted jump per monomer. Afterward the measurements were begun, lasting 20×10^6 MCS. However, the largest system was measured for 200×10^6 MCS. The chain length was 199 segments. Two different densities were investigated, 0.45 and 0.6. The density is defined as the lattice sites occupied divided by the total number of lattice sites. For the lower density, systems with 200 chains in a simulation box of $91 \times 91 \times 91$ grid units, 30 chains in $48 \times 48 \times 48$, 13 chains in $36 \times 36 \times 36$, 4 chains in $24 \times 24 \times 24$, and 1 chain in $15 \times 15 \times 15$ were chosen. The parameters for the higher density were 280 chains in a box of $91 \times 91 \times 91$ and 41 chains in a box of $48 \times 48 \times 48$. All systems were averaged over several independent configurations, the numbers increasing to 200 runs with decreasing segment content in the simulation box, except for the largest one, which was time averaged using about 5×10^6 MCS as the sampling interval. Within the bond-fluctuation model the entanglement length N_e for the low-density systems is about 38 segments and for the high-density systems is 24 segments [18]. Hence the chain length of 200 monomers is about 5.2 N_e and 8 N_e, respectively.

The simulations were run on a Cray-YMP8. The program was vectorized mainly by three means. First, the three-dimensional lattice coordinates were written in a one-dimensional linearized manner. Second, the lattice of the system was divided into cubes of size $7 \times 7 \times 7$ or $6 \times 6 \times 6$, with the exception of the smallest system. In the athermal case a distance of at least 5 grid units ensures that parallel movement of monomers can be performed without their influencing one another. Within each cube the same randomly chosen lattice site was subject to the following vector compression procedure, the third tool. If monomers are found at these sites in the different cubes, these monomers are noted in a list. Next, the possibility of their jumping in a randomly chosen direction is checked. If this is not possible for a certain monomer due to occupation of the site, this monomer is removed from the list.

0021-9991/97 $25.00

Thereafter the list is compressed. For the remaining monomers the existence of the new bond vectors is determined. Another reduction of the list removes all monomers which failed this test. Finally, using this list for addressing, the jumps are performed and the occupation of the lattice sites is updated. With these techniques vector lengths of around 1000 are obtainable for the largest systems. An early implementation of this vectorization procedure together with program listings can be found in the publication of Wittmann and Kremer [19]. The performance, given for the largest simulations, was about 2.2×10^6 MCS per second, resulting in about 90×10^6 vector integer and logical operations per second, 27×10^6 vector floating-point operations per second, and 18×10^6 scalar functional unit operations per second. As this is a lattice-based simulation, most of the calculations can be performed using integer operations and look-up tables, which in itself speeds up the calculations. But this leads to a relatively low portion of floating-point operations in comparison to integer operations. The rate of accepted moves was ca. 12% of the attempted moves.

The resulting dynamics of the chains in the melt was investigated by calculating the mean square displacement $g_1(t)$ of the monomers

$$g_1(t) = \frac{1}{5} \sum_{i=N/2-2}^{N/2+2} \langle [\mathbf{r}_i(t) - \mathbf{r}_i(0)]^2 \rangle, \tag{1}$$

the mean square displacement $g_2(t)$ of the monomers in the center of mass system

$$g_2(t) = \frac{1}{5} \sum_{i=N/2-2}^{N/2+2} \langle [\mathbf{r}_i(t) - \mathbf{r}_{\mathrm{cm}}(t) - (\mathbf{r}_i(0) - \mathbf{r}_{\mathrm{cm}}(0))]^2 \rangle, \tag{2}$$

and the mean square displacement of the center of mass

$$g_3(t) = \langle [\mathbf{r}_{\mathrm{cm}}(t) - \mathbf{r}_{\mathrm{cm}}(0)]^2 \rangle. \tag{3}$$

$\mathbf{r}_i(t)$ is the position of monomer i and $\mathbf{r}_{\mathrm{cm}}(t)$ is the position of the center of mass at time t. The brackets $\langle \cdots \rangle$ denote an average over all chains in the corresponding sample. In Eqs. (1) and (2) only the five innermost monomers of a chain are added to reduce possible chain-end effects [11].

For short chains in a melt $g_1(t)$ should obey the following power laws according to the Rouse model [21, 22]:

$$g_1(t) \sim \begin{cases} t^1: & t < \tau_0 \\ t^{1/2}: & \tau_0 \le t < \tau_{\mathrm{R}} \\ t^1: & t \ge \tau_{\mathrm{R}}. \end{cases} \tag{4}$$

For times shorter than τ_0, the monomer diffuses freely. Afterward the monomer realizes that it belongs to a chain and the dynamics slows down. Beyond $\tau_R \sim N^2$, the largest relaxation time of the chain (the Rouse relaxation time), the monomer diffuses freely again as part of the free diffusing chain. However, for large chains this behavior is modified due to entanglements. In the framework of reptation theory [23, 24] $g_1(t)$ should be described by the following power-law sequence for chains which significantly exceed the critical entanglement length N_{e}:

$$g_1(t) \sim \begin{cases} t^1: & t < \tau_0 & \\ t^{1/2}: & \tau_0 \le t < \tau_{\mathrm{e}} \sim N_{\mathrm{e}}^2 & \text{(a)} \\ t^{1/4}: & \tau_{\mathrm{e}} \le t < \tau_{\mathrm{R}} \sim N^2 & \text{(b)} \\ t^{1/2}: & \tau_{\mathrm{R}} \le t < \tau_{\mathrm{d}} \sim N^3/N_{\mathrm{e}} & \text{(c)} \\ t^1: & \tau_{\mathrm{d}} \le t & \text{(d).} \end{cases} \tag{5}$$

In the new time regimes $\tau_{\mathrm{e}} \le t < \tau_{\mathrm{d}}$ the chain should additionally exhibit a Rouse diffusion along its coarse-grained random walk structure. The chain is confined in a so-called tube built by the surrounding chains. In the regime $\tau_{\mathrm{r}} \le t < \tau_{\mathrm{d}}$ the chain connectivity becomes unimportant for the motion of the segments of the chain, but the tube still confines the segments for another time period. Once the tube disengagement time τ_{d} is reached an overall Einstein diffusion should be observed.

The time regimes for $g_3(t)$ within the reptation model are

$$g_3(t) \sim \begin{cases} t^1: & t < \tau_{\mathrm{e}} & (\alpha) \\ t^{1/2}: & \tau_e \le t < \tau_{\mathrm{d}} & (\beta) \\ t^1: & \tau_{\mathrm{d}} \le t & (\gamma). \end{cases} \tag{6}$$

In Fig. 1, g_1 is displayed for different box sizes. Although the density remains almost constant a qualitative change in the diffusion properties can be found when the box size is reduced to below a certain value. The behavior of systems with 200 and 30 chains in the simulation box is almost indiscernible; the system with 13 chains shows the first differences. The system with only 4 chains exhibits pronounced deviations in long-term properties. No regime with an exponent smaller than 0.45 can be monitored. Instead, a regime with an exponent of 0.6 is found and an early upswing to $\sim t^1$ occurs. The larger samples yield a behavior proportional to about 1/3, change back to 0.5, and finally adopt 1. (For the exponents obtained see Table I.) The unorthodox behavior of the 4-chain system is even more pronounced for only one chain interacting with itself. No slowing could be detected for the self-constrained chain. Hence, the diffusion under the constraints of other chains is not comparable to the constraints due to the same chain. Its connectivity leads a single chain to move in a

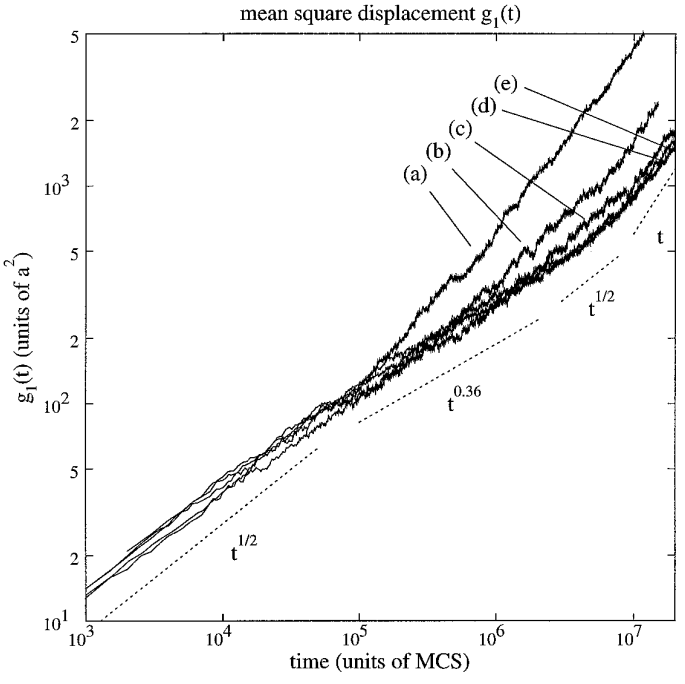

FIG. 1. Mean square displacement g_1 for different box sizes: (a) 1 chain in 15 × 15 × 15, (b) 4 chains in 24 × 24 × 24, (c) 13 chains in 36 × 36 × 36, (d) 30 chains in 48 × 48 × 48, and (e) 200 chains in 91 × 91 × 91.

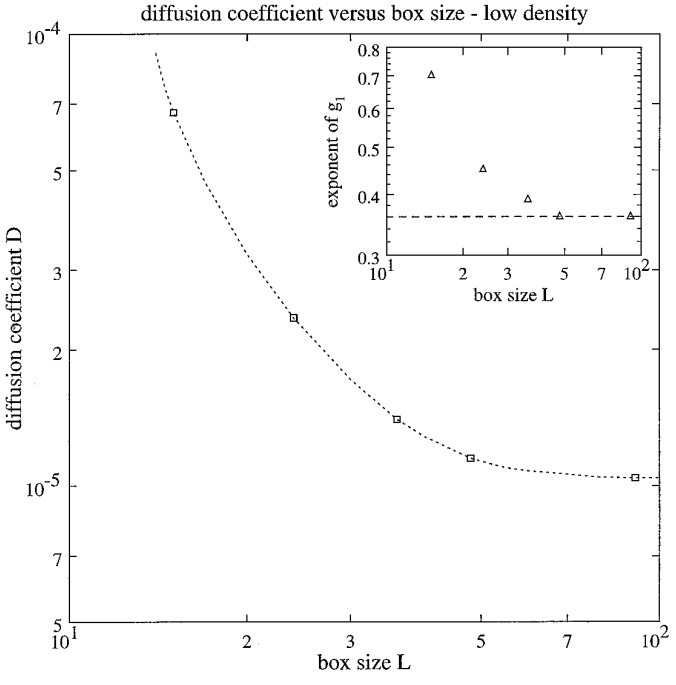

FIG. 2. D versus box size L for the low-density systems. Inset: exponent of $g_1(t)$ in the reptation regime versus L. The dotted line is meant as a guide to the eye.

highly correlated manner. Thus, at least 30 chains consisting of 200 monomers are necessary to resemble the characteristic melt properties. The results in $g_3(t)$ (cf. Table III) confirm the above statements.

To derive further information on finite size effects the diffusion coefficient

$$D = \frac{g_3(t)}{6t} \tag{7}$$

was calculated for the center of mass motion in the time regime of an overall Einstein diffusion. Figure 2 displays the results for the low-density systems with respect to their box sizes. The dotted line is meant as a guide to the eye, showing the possible dependence. No simple power law can be fitted through all points. At box sizes larger than 48 a leveling off toward a constant value seems to occur. The inset in Fig. 2 shows the development of the exponent of $g_1(t)$ in the reptation regime (see above) versus box size. The exponent decreases as the box size grows in the same manner as the diffusion coefficient. This significant decrease in the exponent strongly suggests fundamental changes in the underlying mechanisms of motion. In other words, a self-entangled chain behaves completely differently in comparison to a chain in a melt of many other chains. Once more, our conclusion is that a polymer melt must be modeled as a multichain system in order to obtain true melt properties. Thus, the observed decrease in the diffusion coefficient should not be treated in the classical concept of finite size scaling [20].

The squared radius of gyration, R_g^2, of a chain in the melt, averaged over all chains in the system, is displayed in Fig. 3. In this plot only the last 50 × 10^6 MCS of the total 200 × 10^6 MCS are shown. Despite the preceding relaxation of 150 × 10^6 MCS, R_g^2 fluctuates with an amplitude of 10% of the mean value. This time scale of the fluctuations is around 20 × 10^6 MCS, in close relation to

TABLE I

Exponents of $g_1(t)$ for the Different Regimes: Low Density

Chains	(a)	(b)	(c)	(d)
200	0.50 ± 0.02	0.36 ± 0.01	0.50 ± 0.01	0.94 ± 0.05
30	0.50 ± 0.02	0.36 ± 0.01	0.50 ± 0.01	0.97 ± 0.05
13	0.50 ± 0.02	0.39 ± 0.01	0.50 ± 0.02[a]	0.93 ± 0.05
4	0.50 ± 0.02	0.45 ± 0.01	—[a]	0.98 ± 0.05
1	0.50 ± 0.02	—[b]	—[b]	1.00 ± 0.05

[a] A growing regime with an exponent of 0.60 ± 0.03 can be observed between regimes (c) and (d).

[b] A regime with an exponent of 0.70 ± 0.05 can be observed between regimes (b) and (d).

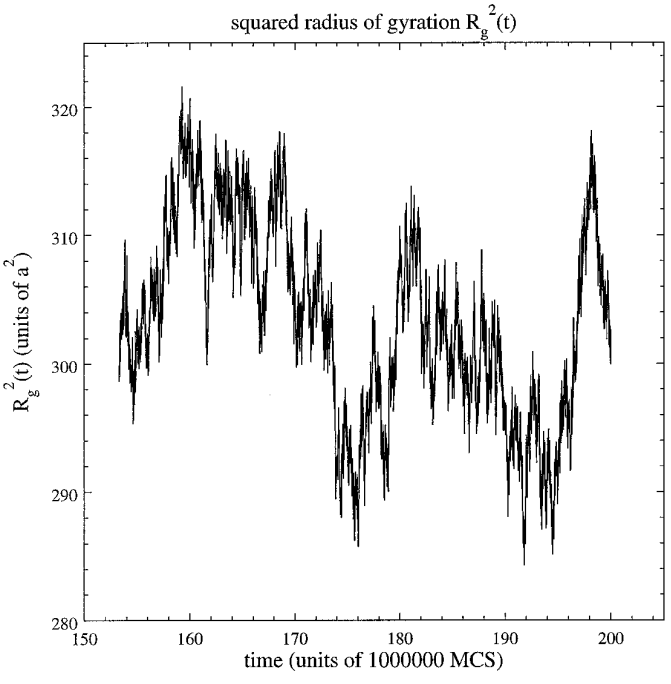

FIG. 3. Squared radius of gyration obtained from the largest system during the final 50×10^6 MCS.

the longest relaxation time, τ_R, in the system. The Rouse time, τ_R, can be found from Fig. 4 roughly at the onset of the second $t^{1/2}$ regime. Thus, when averaging processes are performed for structural properties comparable to common static experimental data, several relaxation time periods must transpire and the averaging must be done over this long period. With this in mind Fig. 1 of the large-scale simulation of Brown *et al.* [15], displaying the squared radius of gyration versus simulation time, is more likely to display the first part of longer-lasting fluctuations. Thus, their conclusion to have reached the steady-state limit should be treated with caution. This is a clear indication that even this profound molecular dynamics simulation ranging up to 8 ns suffers from time limitations.

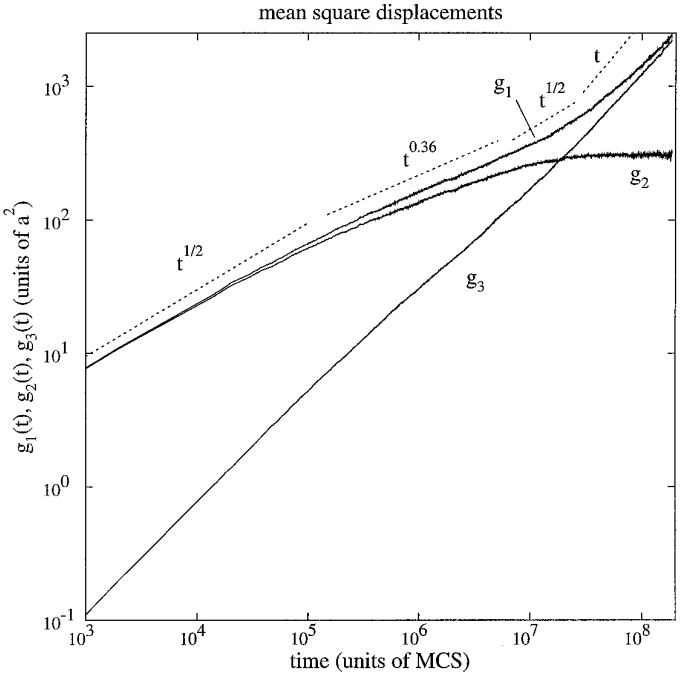

FIG. 4. g_1, g_2, and g_3 for the largest system, 280 chains in $91 \times 91 \times 91$.

TABLE II

Exponents of $g_1(t)$ for the Different Regimes: High Density

Chains	(a)	(b)	(c)	(d)
280	0.50 ± 0.02	0.36 ± 0.01	0.50 ± 0.01	0.90 ± 0.05[a]
41	0.50 ± 0.02	0.37 ± 0.01	0.50 ± 0.01	—[b]

[a] Within the limited simulation time.
[b] Not measured.

There has been a long-lasting discussion on whether or not reptation in polymer melts takes place, experimentally, e.g., [25], computer numerically [18, 26–37], and theoretically [23, 24, 38, 39]. Exponents in the so-called reptation regime were predicted and partially found ranging from 0.25 to 0.40. We cannot provide a conclusive judgment concerning these discussions, but we will attribute our results within the current simulation. Assuming that the dynamics is separable into different time regimes we find the following sequence of exponents for $g_1(t)$, displayed as an example in Fig. 4, summarized in Table I for the low-density system and in Table II for the high-density system. The values for $g_3(t)$ can be found in Tables III and IV.

No exponents smaller than 0.36 were observed; thus no clear evidence for reptation as discussed above is found for the chain lengths investigated. Within the simulations presented, this lack of confirmation of the reptation predic-

TABLE III

Exponents of $g_3(t)$ for the Different Regimes: Low Density

Chains	(α)	(β)	(γ)
200	0.85 ± 0.02	0.73 ± 0.02	0.90 ± 0.02[a]
30	0.88 ± 0.03	0.80 ± 0.01	1.00 ± 0.01
13	0.90 ± 0.02	0.80 ± 0.02	1.00 ± 0.02
4	0.98 ± 0.02	0.95 ± 0.02	1.00 ± 0.02
1	1.00 ± 0.02	1.00 ± 0.02	1.00 ± 0.02

[a] Within the limited simulation time.

TABLE IV

Exponents of $g_3(t)$ for the Different Regimes: High Density

Chains	(α)	(β)	(γ)
280	0.85 ± 0.02	0.74 ± 0.01	0.90 ± 0.02[a]
41	0.85 ± 0.02	0.75 ± 0.01	0.90 ± 0.04[a]

[a] Within the limited simulation time.

tion is independent of density. However, it should be emphasized that the chains investigated are finite chains with the ratio $N/N_e \cong 8$.

Summarizing, in this paper we have presented an investigation of the influence of system size on the dynamical properties of polymer melts. It has been demonstrated that periodic boundary conditions cannot replace a certain minimum system size for a simulation of polymer melts. A further important finding is that long-lasting fluctuations in the radius of gyration on a time scale of the Rouse time exist. Thus, even when determining static properties of melts, at least an averaging over periods larger than several Rouse times is necessary. Unfortunately this implies an increasing amount of CPU time. Furthermore we gave our estimates for the exponents in the different time regimes concerning the reptation problem.

ACKNOWLEDGMENTS

Parts of the simulations were performed at the Leibniz Rechenzentrum der Bayerischen Akademie der Wissenschaften München, Höchstleistungsrechenzentrum für Wissenschaft und Forschung KFA Jülich, and on the facilities of the Rechenzentrum der Universität Regensburg. We are grateful for generous grants of computing time. Moreover M.W. (Go 287/18-1) and T.H. (Go 287/20-1) thank the Deutsche Forschungsgemeinschaft (DFG) for financial support.

REFERENCES

1. S. W. Smith, C. K. Hall, and B. D. Freeman, *Phys. Rev. Lett.* **75,** 1316 (1995).
2. H. L. Trautenberg, M. Wittkop, Th. Hölzl, and D. Göritz, *Phys. Rev. Lett.* **76,** 4448 (1996).
3. S. W. Smith, C. K. Hall, and B. D. Freeman, *Phys. Rev. Lett.* **76,** 4449 (1996).
4. R. J. Roe, D. Rigby, H. Furura, and H. Tukeuchi, *Comput. Polym. Sci.* **2,** 32 (1992).
5. R. J. Roe, *J. Chem. Phys.* **100,** 1610 (1994).
6. M. Hutnik, F. T. Gentile, P. J. Ludovice, U. W. Suter, and A. S. Argon, *Macromolecules* **24,** 5962 (1991).
7. J. Gao and J. H. Weiner, *Macromolecules* **25,** 1349 (1992).
8. M. Wolfgardt, J. Baschnagel, W. Paul, and K. Binder, *Phys. Rev. E* **54,** 1535 (1996).
9. D. Brown and J. H. R. Clarke, *Macromolecules* **24,** 2075 (1991).
10. J. I. McKechnie, R. N. Howard, D. Brown, and J. H. R. Clarke, *Macromolecules* **26,** 198 (1993).
11. K. Kremer and G. S. Grest, *J. Chem. Phys.* **92,** 5027 (1990).
12. J. S. Shaffer, *J. Chem. Phys.* **101,** 4205 (1994).
13. H. L. Trautenberg, J. U. Sommer, and D. Göritz, *J. Chem. Soc. Faraday Trans.* **91,** 2649 (1995).
14. M. Wittkop, Th. Hölzl, S. Kreitmeier, and D. Göritz, *J. Non-Cryst. Solids* **201,** 199 (1996).
15. D. Brown, J. H. R. Clarke, M. Okuda, and T. Yamazaki, *J. Chem. Phys.* **104,** 2078 (1996).
16. H. P. Deutsch and K. Binder, *J. Chem. Phys.* **94,** 2294 (1991).
17. H. L. Trautenberg, Th. Hölzl, and D. Göritz, *Comput. Theor. Polym. Sci.,* **6,** 135 (1996).
18. W. Paul, K. Binder, D. W. Heermann, and K. Kremer, *J. Phys. II* **1,** 37 (1991); *J. Chem. Phys.* **95,** 7726 (1991).
19. H.-P. Wittman and K. Kremer, *Comput. Phys. Commun.* **61,** 309 (1990); **71,** 343 (1992); H.-P. Wittmann, Dissertation (Universität Mainz, 1990).
20. K. Binder, *Ferroelectrica* **73,** 43 (1987).
21. P. E. Rouse, *J. Chem. Phys.* **21,** 1272 (1953).
22. M. Doi and S. F. Edwards, *The Theory of Polymer Dynamics* (Clarendon Press, Oxford, 1988).
23. S. F. Edwards, *Proc. Phys. Soc.* **92,** 9 (1967).
24. P. G. de Gennes, *J. Chem. Phys.* **55,** 572 (1971); *Scaling Concepts in Polymer Physics* (Cornell Univ. Press, Ihaca, NY, 1979).
25. W. W. Gaessley, *Adv. Polym. Sci.* **16,** 1 (1974).
26. A. Baumgärtner and K. Binder, *J. Chem. Phys.* **75,** 2994 (1981).
27. M. Bishop, D. Ceperley, H. L. Frisch, and M. H. Kalos, *J. Chem. Phys.* **76,** 1557 (1982).
28. J. M. Deutsch, *Phys. Rev. Lett.* **49,** 926 (1982).
29. M. Bishop, M. H. Kalos, and H. L. Frisch, *J. Chem. Phys.* **79,** 3500 (1983).
30. K. Kremer, *Macromolecules* **16,** 1632 (1983).
31. A. Baumgärtner, *Annu. Rev. Phys. Chem.* **35,** 419 (1984).
32. C. C. Crabb and J. Kovac, *Macromolecules* **18,** 1430 (1985).
33. C. C. Crabb, D. F. Hoffmann, M. Dial, and J. Kovac, *Macromolecules* **21,** 2230 (1988).
34. A. Kolinski, J. Skolnick, and R. Yaris, *J. Chem. Phys.* **84,** 1922 (1986); **86,** 1567 (1987); **86,** 7164 (1987); **86,** 7174 (1987).
35. J. Skolnick, R. Yaris, and A. Kolinski, *J. Chem. Phys.* **88,** 1407 (1988).
36. J. Wittmer, W. Paul, and K. Binder, *Macromolecules* **25,** 7211 (1992).
37. M. Schulze, R. G. Winkler, and P. Reineker, *Phys. Rev. B* **48,** 581 (1993).
38. M. F. Herman, *J. Non-Cryst. Solids* **131–133,** 715 (1991).
39. K. S. Schweizer and G. Szamel, *Philos. Mag. B* **71,** 783 (1995).

Received June 10, 1996; revised December 16, 1996

Stefan Kreitmeier
Markus Wittkop
Hans L. Trautenberg
Thomas Hölzl
Dietmar Göritz

Institut für Experimentelle und Angewandte Physik
Universität Regensburg
D-93040 Regensburg, Germany